

Use of Pyrolysed Almond and Walnut Shells (PAS and PWS) for the Adsorption of Cationic Dye: Reusing Agro-Waste for Sustainable Development

Gül Kaykioğlu¹ , Nesli Aydın^{1,2*} 

¹ Tekirdağ Namık Kemal University, Faculty of Engineering, Department of Environmental Engineering, Çorlu, Tekirdağ, Türkiye

² Karabük University, Faculty of Engineering, Department of Environmental Engineering, Karabük, Türkiye

*nesli.ciplak.aydin@gmail.com

* Orcid No: 0000-0002-7561-4280

Received: 06 June 2023

Accepted: 10 September 2023

DOI: 10.18466/cbayarfbe.1310461

Abstract

Agro-wastes are recognised as a carbon-rich source, which can be converted into value-added products in sustainable development. In this study, the effect of pH, contact time, initial concentration, and ionic strength were evaluated in Methylene Blue (MB) adsorption by using an activated carbon obtained from pyrolysed almond (PAS) and walnut shells (PWS). The characterisation of PAS and PWS was conducted by SEM-EDX, FT-IR and BET analysis. The removal efficiency of 6 mg/L initial MB concentration improved from 10.6% to 50.42% for PAS, when the adsorbent dose was increased from 0.5 g to 3.5 g/L in 1 L dye solution. It also improved from 14.8% to 48.7% for PWS, when the adsorbent dose was increased from 0.5 g to 3.5 g. The adsorption fits well with the Freundlich isotherm model and the second-order kinetic model is more favourable. In the adsorption experiments using PWS, 48% removal efficiency was obtained in the absence of NaCl. Depending on the increasing NaCl concentration, the removal efficiencies showed a decrease. 36% removal efficiency was obtained for PWS when 2500 mg/L NaCl was used. In the adsorption experiments using PAS, 40% removal efficiency was obtained in the absence of NaCl. When 500 mg/L NaCl was used, the maximum removal efficiency improved to 48%. However, with the increase in ionic strength, removal efficiencies decreased to approximately 39%. This study revealed that PAS and PWS could be used effectively instead of commercial activated carbon, which also provides an advantageous option from an economic point of view.

Keywords: Adsorption, Agro- Waste, Methylene Blue, Removal Efficiency, Sustainable Development

1. Introduction

Agro-waste has recently created new opportunities for the production of eco-friendly and sustainable materials in environmental engineering. As it is cheap and available in large amounts, employing this resource by the direct use or developing, functioning, and/or preparing adsorbents in the adsorption process has been a focus of adsorption studies. Some researchers investigated the use of agro-wastes, such as rice husk, olive stones, fruit stones and nutshells and revealed their high adsorption capacity [1-3]. The performance of H₂SO₄-activated rice husk ash was also studied for the removal of MB and it was determined that the highest adsorption capacity was 44.25 mg/g by reporting that the dye uptake occurred rapidly and the adsorption was improved with longer contact time in all experiments [1]. There have also been further studies examining how

pre-treatment, such as the implementation of pyrolysis, influences the capacity of adsorption. For instance, it was found that pyrolysis temperature affected MB adsorption capacity for activated carbons produced from hazelnut and walnut shells [3]. It was reported in the same study that the release of volatiles during pyrolysis leads removal of non-carbon particles and the enhancement of activated carbon.

When the publications regarding the adsorption process are examined in the literature, it is seen that various studies are focusing on the use of agro-wastes as an adsorbent material for colour removal. However, there is no study particularly concerned with the use of pyrolysed almond (PAS) and walnut shells (PWS), which are produced in large quantities worldwide as walnut and almond easily adapt to different climates. So far, various shells have been analysed to reveal their

reusability for different purposes. For example, the production of bio-oil, which was generated from the pyrolysis of coconut shells, was evaluated under different conditions [4]. Physico-chemical properties of almond shells were characterised to determine appropriate applications to reuse them [5]. Therefore, this study aims to investigate the potential of pyrolysed almond and walnut shells as an adsorbent material in the adsorption process comparatively by evaluating the effect of pH, contact time, initial concentration, and ionic strength. Adsorption kinetics and isotherm models were examined and the characterisation of the adsorbents was conducted by SEM-EDX, FT-IR and BET analyses to explore their morphologic features.

2. Materials and Methods

2.1. Preparation of PAS and PWS

In this study, pyrolysis was applied to almond and walnut shells. The size of the shells was reduced to 2-3 cm in diameter and then subjected to pyrolysis with nitrogen gas at 550°C for 60 minutes. The pyrolysis process was carried out in a downstream fixed bed and throatless type pyrolysis unit. The diameter of the pyrolysis reactor is 170 mm and the length is 750 mm, and the effective height of the reactor is 700 mm. The pyrolysis unit was operated at a speed of 200 kg/m²h [6]. After thinning the pyrolysis product in a porcelain mortar, it was separated according to the pore size by using 2 mm and 1 mm sieves. In this study, adsorbents with pore diameters less than 1 mm were used.

2.2 Analyses

In this study, pH measurements were performed with the WTW pH 315i pH meter. The colour measurement in the supernatants obtained as a result of adsorption studies was carried out in a spectrophotometer (Thermo Spectronic Hellios Aquamate), taking into account the maximum absorbance value of MB (λ_{max} , 670 nm). Absorbance values obtained at different wavelengths were recorded and RES values were calculated [Equation (1)] [7].

$$RES(\lambda) = (A/d).f \quad (1)$$

In Equation 1, “A” (λ) represents absorbance in the water sample at wavelength. “d” (mm) shows the thickness of the tub. While f (f=1000) is a factor to obtain the spectral absorbance in m⁻¹, RES (λ) indicates wavelength chromaticity number in m⁻¹.

The surface properties and chemical characterisation of PAS and PWS were performed by using SEM, FT-IR and BET analyses. SEM (FEI, Quanta FEG 250) and FT-IR (Bruker, Vertex 70 ATR) analyses were run in Tekirdağ Namik Kemal University Central Research Laboratory (Nabiltem). BET (Quantachrome Autosorb 6B) analysis was performed in the MERLAB (Middle East Technical University Central Laboratory).

2.3 Dye Adsorption

MB, which is a cationic dye with strong water-adhesive properties, is used in different industrial areas. In this study, MB (Merck) was used as an adsorbate. The chemical properties of MB are given in Table 1. A 50 mg/L solution was prepared and used for adsorption studies by making dilutions (2-10 mg/L). Adsorption studies were carried out from synthetic solution prepared with MB at different concentrations (2, 4, 6, 8 and 10 mg/L) at different pH conditions (4, 5.8, 7, 9 and 11).

The variation of the colour removal efficiency depending on the ionic strength was evaluated in the solution to which 500, 1000, 1500, 2000 and 2500 mg/L NaCl were added. The adsorption study was carried out in an orbital shaker and sampling was done at 0, 1, 5, 15, 30, 60, 90 and 120 minutes. Collected samples were centrifuged at 4000 rpm for 5 minutes, and then colour measurement was performed.

Table 1. Chemical properties of MB.

Classification number	52015
Solubility in water	%3.55
Solubility in alcohol	%1.48
λ_{max}	665 nm
Molecular weight	319.9 g/mole
Paint group	Thiazine
Ionisation	Acidic

2.4 Adsorption Kinetics

One of the important factors in evaluating the efficiency of adsorption is the determination of the sorption rate. A pseudo-first-order kinetic model and pseudo-second-order kinetic model were applied to analyse the kinetics of MB adsorption.

The Lagergren equation, which is based on a method used to determine the adsorption rate in liquid phase systems, was used in this study to determine the adsorption kinetics [8]. It is one of the most widely used equations in the pseudo-first-order kinetic model. The line drawn on the graph of t versus $\log(qe-qt)$ shows the application of the first-order kinetic equation for the system. The values of qe and k_1 could be determined from the slope of the graph and the cut-off point. “ qe ” is the adsorbed amounts (mg/g) at equilibrium, at time qt , t . The straight line drawn to the slope of the t versus t/qt graph in the adsorption kinetic rate equation in the second-order kinetic model shows the application of the second-order kinetic model equation for the system. qe and k_2 could be determined from the slope of the graph and the cut-off point.

2.5 Adsorption Isotherms

The adsorption capacity at equilibrium was calculated. Langmuir and Freundlich isotherms were applied in this study.

Adsorption continues until equilibrium is established between the adsorbed pollutant concentration and the pollutant concentration remaining in the solution. The adsorption capacity at equilibrium was calculated using Equation 2 [9].

$$qe=(C_0-C_e)V/m \quad (2)$$

In Equation 2, q_e represents the amount of MB (mg/g) adsorbed by each unit of adsorbent at equilibrium. While C_0 shows MB concentration in solution before adsorption (mg/L), C_e indicates MB concentration remaining in solution at equilibrium after adsorption (mg/L). V is a volume of solution (L) and m is an adsorbent dose (g). The equilibrium state could be explained by various isotherm models such as Freundlich and Langmuir which were also used in this study [10].

The Langmuir isotherm is applied to describe monolayer homogeneous adsorption and provides estimation for the highest adsorption capacity. In Langmuir isotherm (C_e/q_e), K_L (L/g), which is the equilibrium constant, and q_{max} (mg/g), which shows the maximum adsorption capacity for monolayer formation are used. To explain the basic characteristics of the Langmuir model, the dimensionless separation factor R_L was used (Equation 3). An R_L value between 0 and 1 indicates favourable adsorption.

$$R_L = \frac{1}{1+K_L \cdot C_0} \quad (3)$$

Freundlich model is also based on an empirical equation used to determine the adsorption density which could occur on the adsorbent surface [11]. In the model, K_F (L/g) is the experimentally calculated adsorption capacity and $1/n_F$ is an adsorption density. The line in the graph which is drawn using $\ln q_e$ vs. $\ln C_e$ values shows compliance with the Freundlich model. The n_F value represents the compatibility of adsorbent and adsorbate. $1/n_F$ and K_F values are calculated from the slope of the obtained line.

3. Results and Discussion

3.1 Characteristics of PAS and PWS

The results of SEM EDX (Energy-Dispersive X-Ray) and FT-IR analyses of PAS and PWS are given in Figure 1. According to the SEM EDX analysis results, there are three elements (C, O, and K) in the surface elemental composition of both adsorbents. The percentage of carbon element, which plays an active role in the removal of pollutants in the adsorption process, was determined as 88.91% for PAS and 92.02% for PWS.

SEM analyses were used to determine the morphological properties of the adsorbent. Surface porosity for PAS and PWS seems suitable for adsorption. A more uniform porosity distribution is observed for PAS, while relatively irregular porosity and rock-like structures are determined for PWS. As temperature increases with high heating rates, various volatile compounds are released. De-volatilization causes morphological changes in biochar followed by the formation of highly porous surface structures of biochar samples [12]. The result of a BET surface area measurement shows that the surface area for PAS is 3.38 m²/g and for PWS is 51.54 m²/g. The SEM images in Figure 1 also support the surface area results.

The FT-IR spectrum was used to determine the frequency deviations of the functional groups in PAW and PWS. As is seen in Figure 1, the spectrum takes place between 400 and 4000 cm⁻¹. Peak points represent broad adsorption bands; 1553, 1409, 1045, 869, 820, 749, 704, 568 cm⁻¹ for PAW and 1554, 1425, 1110, 1050, 869, 804, 751, 446 cm⁻¹ for PWS. It is estimated that this is correlated to the hemicellulosic and cellulosic breakdown reactions and the elimination of O₂, including compounds leading to the release of CO₂. It is also related to H₂O removal reactions, resulting in the generation of amorphous carbon with various degrees of hydrogenation [13]. The bands observed between 1554 and 1409 cm⁻¹ indicate C—C bonds attributed to the conjugated alkene and (or) C—C stretching in the aromatic ring [14]. Bands in the range of 1110 to 1045 cm⁻¹ represent C—C and C—O stretching vibration [6]. The peaks seen at 869-749 cm⁻¹ are indicative of the presence of CO₃ in biochar [15]. The band at 568-446 cm⁻¹ could correspond to the SiO—H vibration.

3.2 Effect of pH on MB Adsorption with PAS and PWS

The pH value of the solution is important in determining the adsorption mechanism. This is due to the change in the surface charge and thus the adsorption capacity of the adsorbents [16]. Adsorption capacities depending on pH for PAS and PWS are shown in Fig. 2 (a). The effect of pH [4, 5.8 (original pH), 7, 9, 11] was evaluated at $C_0 = 6$ mg/L concentration with PAS and PWS. With the increase in the pH of the solution, the q_e values decreased for both adsorbents. The best q_e value for PAS was obtained as 2.93 mg/g at the original pH (5.8), while the highest q_e for PWS was found as 3.19 mg/g at the original pH (5.8).

The surface charge of an adsorbent is related to the pH_{pzc} value. If the pH_{pzc} value is greater than the pH value of the solution, the adsorbent has a positive surface charge, and if the pH_{pzc} value is less than the pH value of the solution, it has a negative surface charge. It is known that the surface charge of the adsorbent will

increase the adsorption efficiency due to the cationic nature of the MB dyestuff. This is due to the repulsions between the cationic dye molecules and the H⁺ ions in the solution. The PH_{pzc} values obtained for pyrolysed almond shells and walnut shells were determined as 5.6 and 5.1, respectively. In this case, if the pH value is

below 5, the adsorption efficiency is expected to be low. For this reason, it is possible to explain the adsorption mechanism with electrostatic attraction. In this study, maximum q_e values were obtained at pH 5.8 (original pH), and therefore the original pH was used in subsequent evaluations.

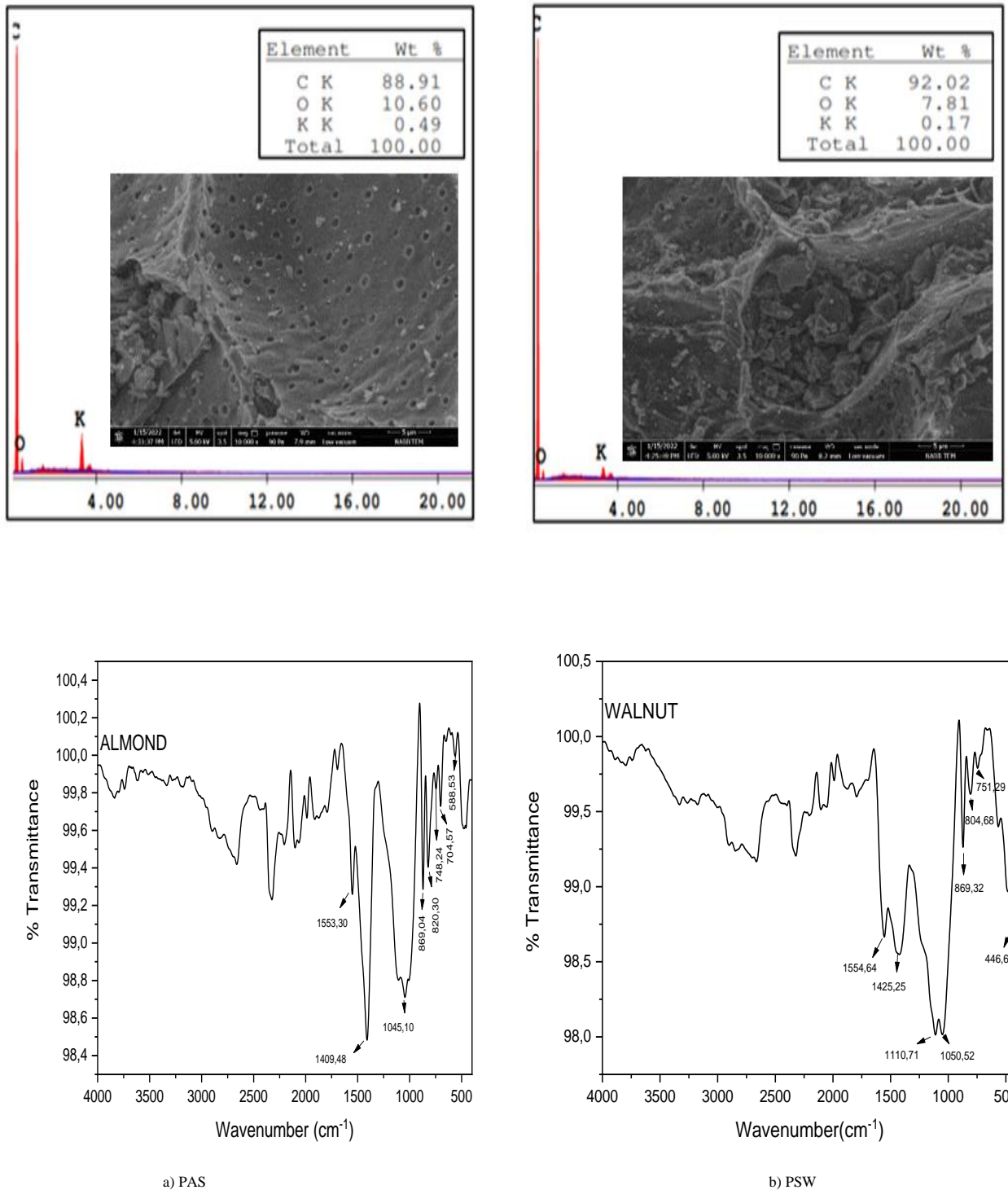


Figure 1. SEM EDX and FT-IR analysis.

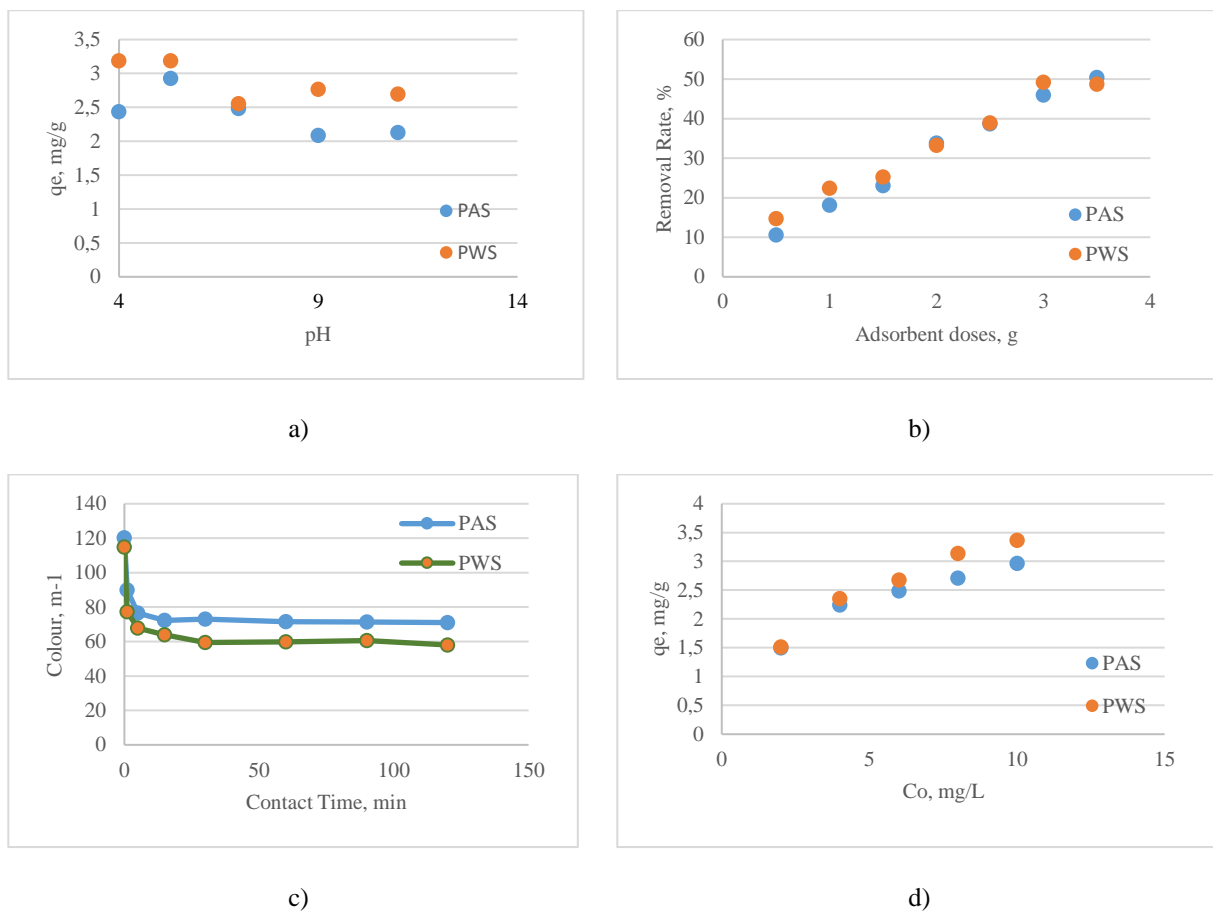


Figure 2. The effect of a) pH, b) adsorbent doses (m), c) contact time ($C_o=6$ mg/L, pH=5.8, $m=2.5$ g/L), d) initial dye concentration (pH=5.8, $m=2.5$ g/L) on dye adsorption with PAS and PWS.

3.3 Effect of PAS and PWS Dose on MB Adsorption

As a result of the MB adsorption study performed with 6 mg/L initial dye concentration and under constant pH conditions, the varying removal efficiencies within 60 minutes of contact time are shown in Figure 2 (b). Accordingly, for both adsorbents, increasing adsorbent doses allowed removal efficiencies to improve. It was determined that approximately 50% colour removal efficiency was obtained in the case of 3.5 g adsorbent application.

3.4 Effect of Contact Time on MB Adsorption by PAS and PWS

The effect of contact time was evaluated for 120 minutes in the case of 6 mg/L initial concentration, original pH (5.8) and 2.5 g/L adsorbent application in 200 mL dye solution. Results are given in Figure 2 (c). According to Figure 2, it is seen that the adsorption takes place rapidly. Depending on the increase in the contact time, the MB concentration in the solution decreases and reaches the equilibrium state at the end of the 60-minute contact period.

3.5 Effect of Initial Dye Concentration on MB Adsorption by PAS and PWS

The effect of initial dye concentration on MB removal with PWS and PAS is shown in Figure 2 (d). An increase in q_e values was observed due to increasing concentrations in adsorption experiments using initial concentrations ranging from 2 mg/L to 10 mg/L, pH 5.8 and fixed adsorbent dose (2.5 g). As it is seen in Figure 2 (d), when C_o is 2mg/L, q_e for both adsorbents was determined as approximately 1.2 mg/g. When C_o was increased to 10 mg/L, the q_e values were determined as 3.36 mg/g and 2.96 mg/g for PWS and PAS, respectively.

3.6 Adsorption Kinetics

In adsorption studies, the time required for the adsorption to reach equilibrium or the rate of adsorption is important to explain the adsorption mechanism. In order to determine the adsorption rate, MB adsorption in PWS and PAS was evaluated using the first-order and second-order kinetic models. The results of the study carried out to explain the adsorption kinetic model are given in Table 2.

When the R^2 values were examined, it was determined that the adsorbents were compatible with both the first-order and the second-order kinetic models. Since the correlation coefficients determined for the second-order kinetic model were higher, it was determined that it was more favourable for the second-order kinetic model. It is seen that the equilibrium adsorption capacities ($q_{e,cal}$) calculated for the second-order kinetic model of both adsorbents are quite compatible with the experimental adsorption capacities ($q_{e,exp}$). The $q_{e,exp}$ and $q_{e,cal}$ values were found as 2.89 mg/g and 3.11 mg/g for PAS, 3.02 mg/g and 3.08 mg/g for PWS, respectively. The rate constants (k_2) determined according to the second-order reaction kinetics were measured as 0.069 and 0.166 m/mg.min for PAS and PWS, respectively. This shows that MB adsorption takes place at a higher rate of PWS compared to PAS.

Table 2. Kinetic parameters for the adsorption of MB by using PAS and PWS ($C_0=6$ mg/L, $m= 2.5$ g/L, $pH=5.8$).

Pseudo-first order					
	C_0	$q_{e, exp}$ (mg/g)	$q_{e, cal}$ (mg/g)	k_1 (min^{-1})	R^2
PAS	6	2.89	1.22	0.007	0.9896
PWS	mg/L	3.02	1.04	0.0099	0.989
Pseudo-second order					
	C_0	$q_{e, exp}$ (mg/g)	$q_{e, cal}$ (mg/g)	k_2 (g/mg min)	R^2
PAS	6	2.89	3.11	0.069	0.9958
PWS	mg/L	3.02	3.08	0.166	0.9975

The q_{max} values obtained in previous studies on MB adsorption are also summarised in Table 3. The MB adsorption capacities of PWS and PAS were determined to be lower than the adsorption capacities of similar adsorbents used in other studies. For instance, a 4-fold difference between the q_{max} values (12.21 mg/g) was obtained in MB adsorption of granular activated carbon and the q_{max} values of PWS and PAS [1]. This shows that approximately 4 times more adsorbent should be used to obtain the same removal efficiency. The fact that the adsorbents (PWS and PAS) to be used instead of commercial activated carbon are waste materials makes the application advantageous from an economic point of view.

Table 3. q_{max} values obtained in studies on MB adsorption.

Adsorbent	q_{max} (mg/g)	Source
Activated Carbon	263.49	[16]
Granular activated carbon	12.21	[1]
Lemon peel	29.0	[17]
Olive stones	22.10	[2]
Nutshell	8.82	[3]
Sunflower seed husk (Helianthus annuus)	23.20	[18]
Spent rice	8.13	[19]
Orange waste	30.3	[20]
PAS	3.02	This study
PWS	3.50	This study

3.7 Adsorption Isotherms

Langmuir and Freundlich isotherms were evaluated by using the data obtained as a result of MB adsorption experiments with PWS and PAS. Isotherm coefficients and correlation coefficients (R^2) are given in Table 4. Langmuir and Freundlich isotherm curves are shown in Figure 3. Considering the R^2 values given in Table 4, the Freundlich model was more favourable for adsorption than the Langmuir model.

In the Freundlich isotherm, the KF value represents the adsorption capacity and the $1/n$ shows the adsorption density or heterogeneity factor [3, 21]. As the heterogeneity of the adsorbent surface increases, the $1/n$ value approaches zero [21]. This indicates the favourability of MB removal.

As is seen in Table 4, the $1/n$ values of MB adsorption for PWS and PAS were determined as 0.20 and 0.17, respectively. This shows that both adsorbents are favourable for MB adsorption [21]. If the adsorption process between an adsorbent and a pollutant is physical, $n > 1$; if it is chemical, then $n < 1$, and if it is linear, $n = 1$ [21]. All n values obtained in this study are greater than 1. For this reason, it can be stated that the adsorption process for both adsorbents is physical adsorption.

Table 4. Isotherm constants for Langmuir and Freundlich isotherms.

	Langmuir			Freundlich			
	Q_{max} (mg/g)	K_L	R^2	K_F	$1/n$	n	R^2
PAS	3.02	2.23	0.992	2.05	0.17	5.88	0.9937
PWS	3.50	1.84	0.9867	2.22	0.20	5	0.9904

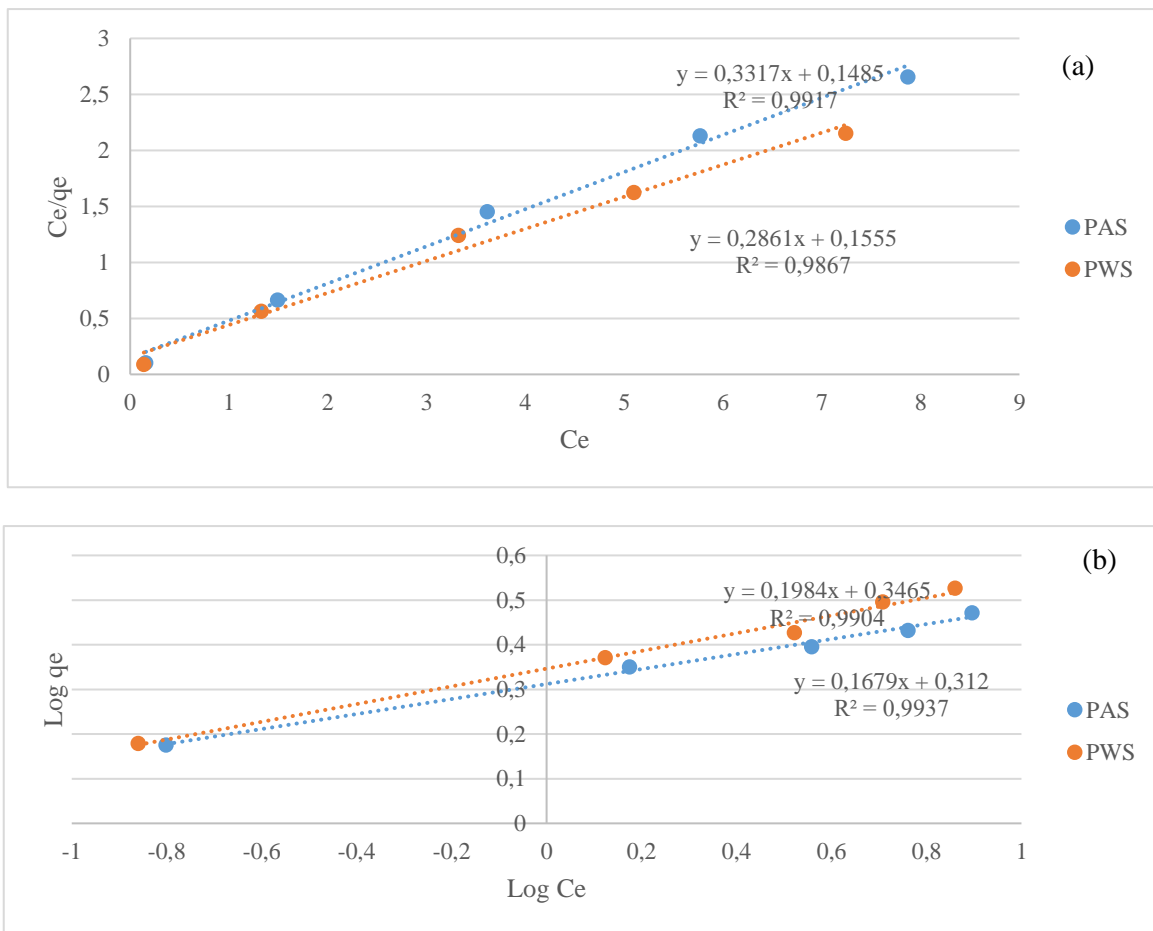


Figure 3. Isotherm Curves a) Langmuir, b) Freundlich (pH = 5.8, t = 60 min, $C_o = 2, 4, 6, 8$ and 10 mg/L, $m = 2.5$ g/L)

3.8 Effect of Ionic Strength on MB Adsorption by PAS and PWS

The effect of ionic strength on MB adsorption with PAS and PWS was examined by adding 500, 1000, 1500, 2000 and 2500 mg/L NaCl into the solution. The removal efficiencies obtained are shown in Figure 4. In the adsorption experiments with PWS, 48% removal efficiency was obtained in the absence of NaCl in the

solution. However, removal efficiencies decreased with increasing NaCl concentration. 36% removal efficiency was obtained with 2500 mg/L NaCl. Increasing the ionic strength in the solution could prevent the electrostatic interaction between the adsorbent surface and the pollutant. It is possible for electrolyte ions to affect potential interfaces on the adsorption surface and to compete for electrolyte ions and adsorbed ions for sorption sites.

In the adsorption experiments made with PAS, an increase in MB removal efficiency was determined in the case of using 500 mg/L NaCl in the solution compared to the case of not using NaCl. This can be explained by the fact that NaCl contributes to the dissociation of the dyestuff into protons and thus positively affects the adsorption. The dyestuff dissociates and becomes more easily adsorbed. Similar results were obtained in some studies [21]. In the

absence of NaCl, 40% removal efficiency was obtained for PAS, while in the case of 500 mg/L NaCl, the removal efficiency improved to 48%. However, with the increase in ionic strength in solution (1000-2000 NaCl mg/L) removal efficiencies were approximately 39%. NaCl concentration was increased up to 2500 mg/L but no significant decrease in removal efficiency was detected.

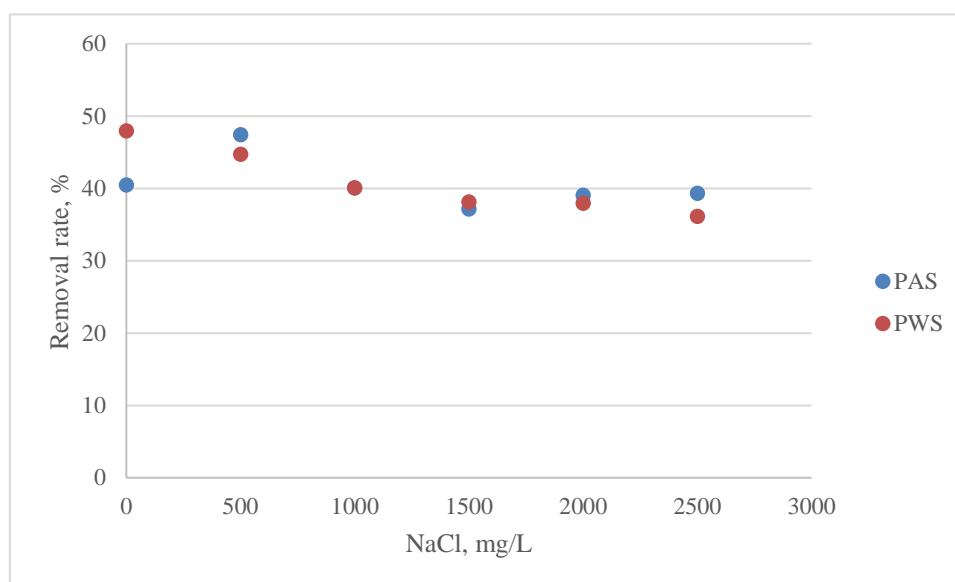


Figure 4. The effect of ionic strength on the adsorption of MB using PAS and PWS ($C_0=6$ mg/L, $m= 2.5$ g/L, $pH=5.8$, $t=60$ min)

4. Conclusion

In this study, the effect of pH, contact time, initial concentration, and ionic strength in MB adsorption were evaluated by using adsorption agents obtained from the pyrolysis of almond and walnut shells. The results of the study are summarised below;

- According to the SEM-EDX results of PAS and PWS used as an adsorbent in the study, the C content was determined as 88.91% and 92.02%, respectively. In addition, according to SEM images, PWS has irregular porosity and rock-like structures, although PAS has a more uniform pore distribution. The result of a BET surface area measurement shows that the surface area for PAS is 3.38 m²/g and for PWS, it is 51.54 m²/g.
- The adsorption efficiency was affected by the initial MB concentration and the adsorbent dose for both adsorbents. The removal efficiency of 6 mg/L initial MB concentration improved from 10.6% to 50.42% for PAS, when the adsorbent dose was increased from 0.5 g to 3.5 g. It also improved from 14.8% to 48.7% for PWS, when the adsorbent dose was increased from 0.5 g to 3.5 g.
- The best q_e value for PAS was obtained as 2.93 mg/g at the original pH (5.8), while the highest q_e for PWS was found as 3.19 mg/g at the original pH (5.8). Depending on the increase in the contact time, the MB concentration in the solution decreases and reaches the equilibrium state at the end of the 60-minute contact period.
- Freundlich isotherm model R^2 values for PWS and PAS used in MB adsorption were found as 0.9904 and 0.9937, respectively. The adsorption process for both adsorbents could be expressed as physical adsorption. It was found that the second-order kinetic model is more favourable to the MB adsorption with PAS and PWS. It was also determined that PWS adsorption took place at a higher rate than PAS.
- A decrease in removal efficiency with PWS was determined due to increasing ionic strength. However, in the case of 500 mg/L NaCl in the solution with PAS, the removal efficiency increased compared to the case of no NaCl. This can be explained by the fact that the salt in the solution dissociates the dyestuffs and facilitates adsorption.

In conclusion, the use of pyrolysed almond and walnut shells in the removal of MB by the adsorption method, which is used in a wide range of industrial activities, was evaluated in this study. It was determined that it is possible to use this adsorbent as an alternative to activated carbon in colour removal. However, due to the low q_{max} values of PAS and PWS compared to activated carbon, a high amount of adsorbent (PAS and PWS) could be required. The q_{max} values can be increased with various chemical activation methods that can be applied to PAS and PWS, and further studies are required on this subject.

Acknowledgement

This research did not receive any specific grant from funding agencies.

Author's Contributions

Nesli Aydın: Drafted and wrote the original manuscript, organised experimental analysis and results.

Gül Kaykioğlu: Supervised experimental work and helped to improve results and discussion.

Ethics

There are no ethical issues after the publication of this manuscript.

Statements and Declarations

This study did not receive any funding. There is no competing interest to declare.

Compliance with ethics guidelines

Ethical approval was not required for the study

References

- [1]. Kaykioğlu, G, Güneş, E. 2016. Kinetic and equilibrium study of methylene blue adsorption using H₂SO₄-activated rice husk ash. *Desalination and Water Treatment*; 57: 7085–7097
- [2]. Alaya, M, Hourieh, M, Youssef, A, El-Sejarah, F. 1999. Adsorption properties of activated carbons prepared from olive stones by chemical and physical activation. *Adsorption Science and Technology*; 18: 27–42
- [3]. Aygun, A., Yenisoy-Karakas, S., Duman, I. 2003. Production of granular activated carbon from fruit stones and nutshells and evaluation of their physical, chemical and adsorption properties. *Microporous Mesoporous Mater.*; 66: 189–195
- [4]. Fardhyanti, DS, Damayanti, A. 2017. Analysis of bio-oil produced by pyrolysis of coconut shell. *International Journal of Chemical and Molecular Engineering*; 11(9).
- [5]. Boulrika, H, El Hajam, M, Hajji Nabih, M, Idrissi Kandri, N, Zerouale, A. 2022. Physico-chemical proprieties of almond residues (shells & hulls) collected from the northern region of Morocco (Fez-Meknes). *Research Square*. <https://doi.org/10.21203/rs.3.rs-1676689/v1>
- [6]. Aktaş, T, Dalmış, S, Tuğ, S, Dalmış, F, Kayışoğlu, B. 2017. Development and testing of a laboratory type gasifier for gasification of paddy straw, *Journal of Tekirdag Agricultural Faculty*; 14(2).
- [7]. Polat, MP. 2018. Atıksularda renk ölçüm metotlarının karşılaştırılması, Master Theses, Hasan Kalyoncu University, Gaziantep, Turkey
- [8]. Garg, VK, Gupta, R, Yadav, AB, Kumar, R. 2003. Dye removal from aqueous solution by adsorption on treated sawdust. *Bioresource Technology*. [https://doi.org/10.1016/S0960-8524\(03\)00058-0](https://doi.org/10.1016/S0960-8524(03)00058-0)
- [9]. Aldemir, A, Kul, AR. 2020. Comparison of Acid Blue 25 adsorption performance on natural and acid-thermal co-modified bentonite: Isotherm, kinetics and thermodynamics studies. *Pamukkale University Journal of Engineering Sciences*; 26: 1335-1342.
- [10]. Kaykioğlu, G, Güneş, E. 2016. Comparison of Acid Red 114 dye adsorption by Fe₃O₄ and Fe₃O₄ impregnated rice husk ash. *Journal of Nanomaterials*; 6304096. <https://doi.org/10.1155/2016/6304096>
- [11]. El-Halwany, MM. 2010. Study of adsorption isotherms and kinetic models for Methylene Blue adsorption on activated carbon developed from Egyptian rice hull (Part II), *Desalination*, <https://doi.org/10.1016/j.desal.2008.07.030>
- [12]. Alfattani, R, Shah, MA, Siddiqui, MIH, Ali, MA, Alnaser, IA. 2022. Bio-Char characterization produced from walnut shell biomass through slow pyrolysis: Sustainable for soil amendment and an alternate bio-fuel, *Energies*. doi: <https://doi.org/10.3390/en15010001>
- [13]. Genieva, S, Gonsalvesh, L, Georgieva, V, Tavlieva, M, Vlaev, L. 2021. Kinetic analysis and pyrolysis mechanism of raw and impregnated almond shells. *Thermochimica Acta*; 698, 178877
- [14]. Farges, R, Gharzouni, A, Ravier, B, Jeulin, P, Rossignol, S. 2018. Insulating foams and dense geopolymers from biochar by-products. *Journal of Ceramic Science and Technology*; 2(9): 193-200. 10.4416/JCST2017-00098
- [15]. Shofiyani, A, Gusrizal. 2006. Determination of pH effect and capacity of heavy metals adsorption by water hyacinth (Eichhornia Crassipes) biomass, *Indonesian Journal of Chemistry*; 6(1): 56-60.
- [16]. Li, Y, Du, Q, Liu, T, Peng, X, Wang, J, Sun, J, Wang, Y, Wu, S, Wang, Z, Xia, Y, Xia, L. 2013. comparative study of methylene blue dye adsorption onto activated carbon, graphene oxide, and carbon nanotubes. *Chemical Engineering Research and Design*; 91: 361–368
- [17]. Kumar, KV, Porkodi, K. 2006. Relation between some two- and three-parameter isotherm models for the sorption of Methylene Blue onto lemon peel. *Journal of Hazardous Materials*; 138: 633–635
- [18]. Ong, ST, Keng, PS, Lee, SL, Leong, MH, Hung, YT. 2010. Equilibrium studies for the removal of basic dye by sunflower seed husk (Helianthus annuus). *International Journal of the Physical Sciences*; 5, 1270.
- [19]. Rehman, MSU, Kim, I, Han, JI. 2012. Adsorption of methylene blue dye from aqueous solution by sugar extracted spent rice biomass. *Carbohydrate Polymers*; 90: 1314-1322
- [20]. Irem, S, Khan, QM, Islam, E, Hashmat, AJ, ul Haq, MA, Afzal, M, Mustafa, T. 2013. Enhanced removal of reactive navy blue dye using powdered orange waste. *Ecological Engineering*. 58: 399-405
- [21]. Wu, Z, Zhong, H, Yuan, X, Wang, H, Wang, L, Chen, X, Zeng, G, Wu, Y. 2014. Adsorptive removal of methylene blue by rhamnolipid-functionalized graphene oxide from Wastewater. *Water Research*; 67: 330-344